Magnetic Geometric Dynamics Around Ioffe-Ştefănescu Configuration

C. Udrişte

Abstract

Section 1 recalls the ideas of Ioffe about realization of a magnetic trap for plasma confinement and the ideas of Ştefănescu about the morphology of elementary magnetic fields. Section 2 gives the components of the magnetic field around Ioffe-Ştefănescu configuration, and their trapezoidal or Gauss approximations. Section 3 describes the Lagrangian and Hamiltonian approaches of the continuous or discrete magnetic geometric dynamics. Section 4 includes 19 annotated MAPLE 6 worksheets regarding the morphology of the magnetic field around Ioffe-Ştefănescu configuration. All these simulations predict a magnetic trap feasible without special technology.

Mathematics Subject Classification: 70H03, 70H05, 78H35, 65P10

Key words: magnetic field, magnetic trap, Ioffe-Stefanescu configuration, numerical procedures, magnetic geometric dynamics, MAPLE 6 worksheets, Euler-Lagrange equations, Hamilton equations.

1 Ioffe-Ştefănescu Magnetic Trap

In the period 1925-1994 Sabba Ştefănescu [7]-[33] drew attention that the morphology of the magnetic fields generated by currents through union of piecewise rectilinear electric circuits is not yet well understood or applied. Its papers show that this morphology comes from the geometry of electric configuration, and not from continuity (discontinuity) of the generating electric field or circuits. Also they eliminate the wrong idea that "a system of two equal infinite rectilinear currents cannot constitute by any means a closed circuit". This objection is now fully grounded. But, if it is admitted that the two "currents" (straight lines) are closed at infinity through filiform rectilinear junctions, one may prove easily that these junctions determine, within large finite distance, a neglijible contribution to the magnetic field, and consequently, this part of the field cannot modify the paternity of the morphology.

Editor Gr.Tsagas *Proceedings of the Conference of Geometry and Its Applications in Technology and The Workshop on Global Analysis, Differential Geometry and Lie Algebras, 1999*, 243-265

On the other hand, in 1962, M.S. Ioffe [3], [4] first reported on plasma-confinement experiments in a magnetic field that increases in every direction away from the plasma boundary, and that did not have the undesirable feature of a region where the magnetic field went to zero inside the plasma.

The magnetic trap used in Ioffe's experiments was created by superposing two magnetic fields: a magnetic mirror field produced by two circular circuits (coils), carrying current in the directions shown in the Fig.1; the field produced by six conductors parallel to the magnetic mirror axis, carrying current in the directions shown in the Fig.1. The two end loops of currents produce the mirror field; the six straight lines of current produce the Ioffe-Ştefănescu improvement (this replaces a piecewise rectilinear circuit consisting of nine segments and two semilines, two by two determining a right angle). That such a field has the feature of increasing the density of magnetic energy $\bar{H}^2$ in every direction away from the plasma, with a nonzero minima in the interior of plasma, can be seen by considering the effect of each of the two fields separately (Figs.4-7).

Remark. Like for any harmonic function, the critical points of $\bar{H}^2$ (if they exists!) are only minima or saddle points.

The magnetic mirror field $\bar{H}_m$ by itself has the properties that the density of magnetic energy $\bar{H}_m^2$ increases as a function of distance along the axis from the midplane (stabilizing), but decreases as a function of distance along a radius from the midplane (destabilizing). On the other hand, the field $\bar{H}_{pw}$ produced by the six parallel conductors leads to the density of magnetic energy $\bar{H}_{pw}^2$ which increases as a function of distance along a radius from the midplane (stabilizing) and is constant along the mirror axis. These combined fields, if properly chosen, have the property that the magnetic field strength $\sqrt{\bar{H}_m^2 + \bar{H}_{pw}^2}$ increases in every direction away from a sphere centered at the midplane origin. To simulate this behaviour, we use an approximation of the magnetic field and MAPLE 6 facilities to produce phase portraits, field surfaces, level sets of $\bar{H}^2$, minimum of $\bar{H}^2$, trajectories in magnetic geometric dynamics, etc.

To prove that the hydromagnetic instability could be supressed with a field configuration in Fig.1, Ioffe and his coworkers at the Kurchatov Institute of Moscow made experiments using the following data:

- a magnetic mirror field with 5,000 G at the midplane and 8,500 G at the mirror peaks,
- a vacuum chamber with the diameter $d = 40$ cm,
- a separation between mirror peaks of $3d = 120$ cm,
- 6 conductors creating the stabilizing multipole magnetic field, situated outside the vacuum chamber, and producing a magnetic field of up 4,500 G at the wall of the vacuum chamber.

From our point of view, in order to describe a magnetic field able to create a magnetic trap, it is enough to judge on the configuration in the Fig.1, with $d = 2cm$, $3d = 6cm$. The magnetic field around this configuration has the components from Section 2 (neglecting a multiplicative factor for the six straight lines, and a multiplicativ factor for the two circles):

2 Magnetic Field Around Ioffe-Ştefănescu Configuration

The magnetic field produced around the electric circuit γ_α, $\alpha = 1, \ldots, p$, is given by the Biot-Savart-Laplace formula

$$\bar{H}_\alpha(x) = \int_{\gamma_\alpha} \frac{\bar{J}_\alpha \times \overline{px}}{px^3} d\tau_p, \quad \forall x = (x_1, x_2, x_3) \in \mathbf{R}^3 \setminus \gamma_\alpha,$$

where $p \in \gamma_\alpha$ is the arbitrary point on the electric circuit γ_α, and $\bar{J}_\alpha$ is the conduction current density (theoretically like the versor $\dot{\gamma}_\alpha$) on γ_α. This magnetic field is irrotational ($rot\ \bar{H}_\alpha = 0$) and solenoidal ($div\ \bar{H}_\alpha = 0$). Also the set $\{\bar{H}_\alpha,\ \alpha = 1, \ldots, p\}$ determines a Lie subalgebra of solenoidal vector fields. The (total) magnetic field produced around the configuration $\Gamma = \bigcup_{\alpha=1}^{p} \gamma_\alpha$ is

$$\bar{H}(x) = \sum_{\alpha=1}^{p} \bar{H}_\alpha(x), \quad x \in R^3 \setminus \Gamma.$$

Let us consider the Ioffe-Ştefănescu configuration of Fig.1. The magnetic field around the hexapole winding $l_1 \cup l_2 \cup l_3 \cup l_4 \cup l_5 \cup l_6$ is $\bar{H}_{pw} = \sum_{i=1}^{6} \bar{H}_i$, where

$$\bar{H}_i = \varepsilon_i \frac{-(y - \sin t_i)\bar{\imath} + (x - \cos t_i)\bar{\jmath}}{(x - \cos t_i)^2 + (y - \sin t_i)^2}, \; i = 1, 2, 3, 4, 5, 6$$

$$\varepsilon_i = \begin{cases} 1 & \text{for} \quad i = \text{even} \\ -1 & \text{for} \quad i = \text{odd} \end{cases}$$

and

t	0	$\pi/3$	$2\pi/3$	π	$4\pi/3$	$5\pi/3$
$\cos t$	1	$1/2$	$-1/2$	-1	$-1/2$	$1/2$
$\sin t$	0	$\sqrt{3}/2$	$\sqrt{3}/2$	0	$-\sqrt{3}/2$	$-\sqrt{3}/2$

Consequently the magnetic field $\bar{H}_{pw}$ has the components

$$H_x = \frac{y}{(x-1)^2 + y^2} - \frac{y - \sqrt{3}/2}{(x - 1/2)^2 + \left(y - \sqrt{3}/2\right)^2} +$$

$$+ \frac{y - \sqrt{3}/2}{(x + 1/2)^2 + \left(y - \sqrt{3}/2\right)^2} - \frac{y}{(x+1)^2 + y^2} +$$

$$+ \frac{y + \sqrt{3}/2}{(x + 1/2)^2 + \left(y + \sqrt{3}/2\right)^2} - \frac{y + \sqrt{3}/2}{(x - 1/2)^2 + \left(y + \sqrt{3}/2\right)^2},$$

$$H_y = -\frac{x-1}{(x-1)^2+y^2} + \frac{x-1/2}{(x-1/2)^2+(y-\sqrt{3}/2)^2} +$$
$$-\frac{x+1/2}{(x+1/2)^2+(y-\sqrt{3}/2)^2} + \frac{x+1}{(x+1)^2+y^2} -$$
$$-\frac{x+1/2}{(x+1/2)^2+(y+\sqrt{3}/2)^2} + \frac{x-1/2}{(x-1/2)^2+(y+\sqrt{3}/2)^2},$$
$$H_z = 0.$$

The magnetic field around the mirror coil $C1 \cup C2$ is $\bar{H}_m = \bar{H}_{C1} + \bar{H}_{C2}$. On the other hand the circle $C1 : x^2+y^2 = 1$, $z = -3$ must be parametrized by the equations $x = \cos t$, $y = \sin t$, $z = -3$, $t \in [0, 2\pi]$, with the tangent versor $\bar{v} = -\sin t\bar{\imath} + \cos t\bar{\jmath}$. Applying Biot-Savart-Laplace formula we find the magnetic field $\bar{H}_{C1}$ around $C1$, of components

$$H_x = (z+3)\int_0^{2\pi} \frac{\cos t}{\varphi(t;x,y,z)}dt$$
$$H_y = (z+3)\int_0^{2\pi} \frac{\sin t}{\varphi(t;x,y,z)}dt$$
$$H_z = -\int_0^{2\pi} \frac{x\cos t + y\sin t - 1}{\varphi(t;x,y,z)}dt,$$

where

$$\varphi(t;x,y,z) = (x^2+y^2+(z+3)^2 - 2x\cos t - 2y\sin t + 1)^{3/2}.$$

These components can be expressed by the elliptic functions.

Analogously, $C2 : x^2+y^2 = 1$, $z = 3$ must be parametrized by the equations $x = \cos t$, $y = -\sin t$, $z = 3$, $t \in [0, 2\pi]$, having the tangent versor $\bar{v} = -\sin t\bar{\imath} - \cos t\bar{\jmath}$. The magnetic field $\bar{H}_{C_2}$ around C_2 has the components

$$H_x = -(z-3)\int_0^{2\pi} \frac{\cos t}{\psi(t;x,y,z)}dt$$
$$H_y = (z-3)\int_0^{2\pi} \frac{\sin t}{\psi(t;x,y,z)}dt$$
$$H_z = \int_0^{2\pi} \frac{x\cos t - y\sin t - 1}{\psi(t;x,y,z)}dt,$$

where

$$\psi(t;x,y,z) = (x^2+y^2+(z-3)^2 - 2x\cos t + 2y\sin t + 1)^{3/2}.$$

Also, these components can be written using elliptic functions.

Instead of using elliptic functions, we prefer the numerical estimations of the integrals in two ways:

- by the trapezoidal rule with 13 points;

- by the Gauss quadrature formula with 3 points.

The numerical procedures for evaluating the previous integrals (with parameters) did not alterate the quality of representing an irrotational and solenoidal magnetic field.

We start with trapezoidal rule using the division of $[0, 2\pi]$ in twelve subintervals as in the table

t	0	$\pi/6$	$\pi/3$	$\pi/2$	$2\pi/3$	$5\pi/6$	π
$\cos t$	1	$\sqrt{3}/2$	$1/2$	0	$-1/2$	$-\sqrt{3}/2$	-1
$\sin t$	0	$1/2$	$\sqrt{3}/2$	1	$\sqrt{3}/2$	$1/2$	0

t	$7\pi/6$	$4\pi/3$	$3\pi/2$	$5\pi/3$	$11\pi/6$	2π
$\cos t$	$-\sqrt{3}/2$	$-1/2$	0	$1/2$	$\sqrt{3}/2$	1
$\sin t$	$-1/2$	$-\sqrt{3}/2$	-1	$-\sqrt{3}/2$	$-1/2$	0

This produces the following approximation of the magnetic field around the mirror coil:

$$\begin{aligned}
H_x &= \frac{\pi}{6}(z+3)\left[\frac{1}{(x^2+y^2+(z+3)^2-2x+1)^{3/2}}+\right.\\
&+ \left.\sum_{j=1}^{11}\frac{\cos t_j}{(x^2+y^2+(z+3)^2-2x\cos t_j-2y\sin t_j+1)^{3/2}}\right]-\\
&- \frac{\pi}{6}(z-3)\left[\frac{1}{(x^2+y^2+(z-3)^2-2x+1)^{3/2}}+\right.\\
&+ \left.\sum_{j=1}^{11}\frac{\cos t_j}{(x^2+y^2+(z-3)^2-2x\cos t_j+2y\sin t_j+1)^{3/2}}\right],
\end{aligned}$$

$$\begin{aligned}
H_y &= \frac{\pi}{6}(z+3)\sum_{j=1}^{11}\frac{\sin t_j}{(x^2+y^2+(z+3)^2-2x\cos t_j-2y\sin t_j+1)^{3/2}}+\\
&+ \frac{\pi}{6}(z-3)\sum_{j=1}^{11}\frac{\sin t_j}{(x^2+y^2+(z-3)^2-2x\cos t_j+2y\sin t_j+1)^{3/2}},
\end{aligned}$$

$$\begin{aligned}
H_z &= -\frac{\pi}{6}\left[\frac{x-1}{(x^2+y^2+(z+3)^2-2x+1)^{3/2}}+\right.\\
&+ \left.\sum_{j=1}^{11}\frac{x\cos t_j+y\sin t_j-1}{(x^2+y^2+(z+3)^2-2x\cos t_j-2y\sin t_j+1)^{3/2}}\right]+\\
&+ \frac{\pi}{6}\left[\frac{x-1}{(x^2+y^2+(z-3)^2-2x+1)^{3/2}}+\right.\\
&+ \left.\sum_{j=1}^{11}\frac{x\cos t_j-y\sin t_j-1}{(x^2+y^2+(z-3)^2-2x\cos t_j+2y\sin t_j+1)^{3/2}}\right].
\end{aligned}$$

By addition we obtain an approximation $\bar{H}_{Tr}$ of the total magnetic field around Ioffe-Ştefănescu configuration $l_1 \cup l_2 \cup l_3 \cup l_4 \cup l_5 \cup l_6 \cup C1 \cup C2$. The magnetic field $\bar{H}_{Tr}$ has a nonzero minima in the interior of the configuration, and a nonzero saddle-critical value in the center of configuration (Figs.4-5).

Alternatively, let us use the Gauss quadrature formula with 3 points,

$$\begin{aligned}\int_0^{2\pi} u(t)dt &= \pi \int_{-1}^{1} u(\pi(1+s))ds = \\ &= \frac{\pi}{9}\left[5u(t_1) + 8u(t_2) + 5u(t_3)\right],\end{aligned}$$

$$t_1 = \pi\left(1 - \sqrt{3/5}\right),\ t_2 = \pi,\ t_3 = \pi\left(1 + \sqrt{3/5}\right),$$

for the approximate evaluation of the magnetic field around the mirror coil. We find

$$\begin{aligned}H_x &= \frac{\pi(z+3)}{9}\left[\frac{5\cos t_1}{\varphi(t_1;x,y,z)} - \frac{8}{\varphi(\pi;x,y,z)} + \frac{5\cos t_3}{\varphi(t_3;x,y,z)}\right] - \\ &- \frac{\pi(z-3)}{9}\left[\frac{5\cos t_1}{\psi(t_1;x,y,z)} - \frac{8}{\psi(\pi;x,y,z)} + \frac{5\cos t_3}{\psi(t_3;x,y,z)}\right],\end{aligned}$$

$$\begin{aligned}H_y &= \frac{5\pi(z+3)}{9}\left[\frac{\sin t_1}{\varphi(t_1;x,y,z)} + \frac{\sin t_3}{\varphi(t_3;x,y,z)}\right] + \\ &+ \frac{5\pi(z-3)}{9}\left[\frac{\sin t_1}{\psi(t_1;x,y,z)} + \frac{\sin t_3}{\psi(t_3;x,y,z)}\right],\end{aligned}$$

$$\begin{aligned}H_z &= -\frac{\pi}{9}\left[5\frac{x\cos t_1 + y\sin t_1 - 1}{\varphi(t_1;x,y,z)} - 8\frac{x+1}{\varphi(\pi;x,y,z)} + 5\frac{x\cos t_3 + y\sin t_3 - 1}{\varphi(t_3;x,y,z)}\right] + \\ &+ \frac{\pi}{9}\left[5\frac{x\cos t_1 - y\sin t_1 - 1}{\psi(t_1;x,y,z)} - 8\frac{x+1}{\psi(\pi;x,y,z)} + 5\frac{x\cos t_3 - y\sin t_3 - 1}{\psi(t_3;x,y,z)}\right].\end{aligned}$$

By addition we obtain another approximation $\bar{H}_{Ga}$ of the total magnetic field around Ioffe-Ştefănescu configuration $l_1 \cup l_2 \cup l_3 \cup l_4 \cup l_5 \cup l_6 \cup C1 \cup C2$. The magnetic field $\bar{H}_{Ga}$ has a nonzero minima in the interior of the configuration, and a nonzero saddle-critical value in the center of configuration (Figs.6-14).

3 Magnetic Geometric Dynamics

The continuous and discrete single-time geometric dynamics is based on a new variant of Lorentz law discovered by us [35], [43], [38], [40]:

a vector field and a Riemannian metric produce a dynamics (single-time geometric dynamics), described by the "rot" of the field and the "grad" of the energy density, whose trajectories are harmonic maps including the trajectories of the vector field.

Consequently, if we want to refer to the dynamical properties of a vector field we must have in mind that the vector field is not alone, but it is accompanied by the geometrical structure of the space, both producing the energy density and the "rot".

Particularly, the continuous and discrete single-time geometric magnetic dynamics is produced on $(R^3 \setminus \Gamma, \delta_{ij})$ by the total magnetic field $\bar{H} = (H_1, H_2, H_3)$.

The continuous magnetic geometric dynamics is described by the DEs system

$$\frac{d^2 x_i}{dt^2} = \frac{\partial f}{\partial x_i},\ i = 1,2,3;\ x = (x_1, x_2, x_3), \tag{1}$$

where $f = \frac{1}{2}(H_1^2 + H_2^2 + H_3^2)$ is the density of magnetic energy.

Theorem. *1) The DEs system* (1) *describes the extremals of the Lagrangians*

$$L_1 = \frac{1}{2}\sum_{i=1}^{3}\left(\frac{dx_i}{dt}\right)^2 - \sum_{i=1}^{3} H_i \frac{dx_i}{dt} + f, \quad L_2 = \frac{1}{2}\sum_{i=1}^{3}\left(\frac{dx_i}{dt}\right)^2 + f$$

as potential maps of the Riemann manifold $(R \times R^3, 1 + \delta)$.

2) The Lagrangians L_1 and L_2 produce the same Hamiltonian

$$\mathcal{H}_1 = \mathcal{H}_2 = \frac{1}{2}\sum_{i=1}^{3}\left(\frac{dx_i}{dt}\right)^2 - f.$$

3) The Lagrangian L_1 defines the generalized impulses

$$p_i = \frac{\partial L_1}{\partial y_i} = y_i - H_i, \quad y_i = \frac{dx_i}{dt},$$

and consequently $\mathcal{H}_1 = \frac{1}{2}\delta^{ij} p_i p_j + \delta^{ij} p_i H_j$.

The Lagrangian L_2 defines the generalized impulses

$$p_i' = \frac{\partial L_2}{\partial y_i} = y_i,$$

and consequently

$$\mathcal{H}_2 = \frac{1}{2}\delta^{ij} p_i' p_j' - f.$$

4) The Hamiltonian vector fields

$$\begin{pmatrix} \dfrac{\partial \mathcal{H}_1}{\partial p_k} \\ -\dfrac{\partial \mathcal{H}_1}{\partial x_k} \end{pmatrix} = \begin{pmatrix} p_k + H_k \\ -\delta^{ij} p_i \dfrac{\partial H_j}{\partial x_k} \end{pmatrix}$$

and

$$\begin{pmatrix} \dfrac{\partial \mathcal{H}_2}{\partial p_k'} \\ -\dfrac{\partial \mathcal{H}_2}{\partial x_k'} \end{pmatrix} = \begin{pmatrix} p_k' \\ \dfrac{\partial f}{\partial x_k'} \end{pmatrix}$$

are related via the diffeomorphism

$$x_i' = x_i, \quad p_i' = p_i + H_i.$$

Proof. 1) The basic relation that transforms the Euler-Lagrange equations $\frac{\partial L_1}{\partial x_k} - \frac{d}{dt}\frac{\partial L_1}{\partial y_k} = 0$, $k = 1, \dots, n$, $y_k = \frac{dx_k}{dt}$, in the equations (1) is $rot\ \bar{H} = 0$.

2) We use the formula $\mathcal{H} = y^i \frac{\partial L}{\partial y_i} - L$.

4) It is enough to check the formula of changing the components of a vector field when we change the coordinates:

$$\begin{pmatrix} \delta_{ji} & 0 \\ \frac{\partial H_j}{\partial x_i} & \delta_{ji} \end{pmatrix} \begin{pmatrix} p_j + H_j \\ -\sum_k p_k \frac{\partial H_k}{\partial x_j} \end{pmatrix} =$$

$$= \begin{pmatrix} p_i + H_i \\ \sum_j (p_j + H_j)\frac{\partial H_j}{\partial x_i} - \sum_k p_k \frac{\partial H_k}{\partial x_i} \end{pmatrix} = \begin{pmatrix} p_i' \\ \frac{\partial f}{\partial x_i'} \end{pmatrix}.$$

Let us accept that the discrete magnetic geometric dynamics is governed by the discrete Lagrangian

$$L_d(x[k-1], x[k]) = \frac{1}{2}\sum_{i=1}^{3}(x_i[k] - x_i[k-1])^2 -$$

$$-h\sum_{i=1}^{3} H_i\left(\frac{x[k] + x[k-1]}{2}\right)(x_i[k] - x_i[k-1]) + h^2 f\left(\frac{x[k] + x[k-1]}{2}\right).$$

Using the general form of the variational integrator [43], we write the discrete Euler-Lagrange equations as follows

$$x_i[k+1] - x_i[k] + \frac{h}{2}\sum_{s=1}^{3}\frac{\partial H_s}{\partial x_i}\left(\frac{x[k+1] + x[k]}{2}\right)(x_s[k+1] - x_s[k]) -$$

$$-hH_i\left(\frac{x[k+1] + x[k]}{2}\right) - \frac{h^2}{2}\frac{\partial f}{\partial x_i}\left(\frac{x[k+1] + x[k]}{2}\right) - A_i[k] = 0,$$

where the term $A_i[k]$ has the following expression

$$A_i[k] = x_i[k] - x_i[k-1] - \frac{h}{2}\sum_{s=1}^{3}\frac{\partial H_s}{\partial x_i}\left(\frac{x[k] + x[k-1]}{2}\right)(x_s[k] - x_s[k-1]) -$$

$$-hH_i\left(\frac{x[k] + x[k-1]}{2}\right) + \frac{h^2}{2}\frac{\partial f}{\partial x^i}\left(\frac{x[k] + x[k-1]}{2}\right).$$

Of course, if we denote

$$\varphi_i(u) = u_i - x_i[k] + \frac{h}{2}\sum_{s=1}^{3}\frac{\partial H_s}{\partial x_i}\left(\frac{u+x[k]}{2}\right)(u_s - x_s[k]) -$$
$$-hH_i\left(\frac{u+x[k]}{2}\right) - \frac{h^2}{2}\frac{\partial f}{\partial x_i}\left(\frac{u+x[k]}{2}\right) - A_i[k],$$

the discrete solution is obtained by solving at each step k, the system of equations $\varphi_i(u) = 0$, $i = 1, 2, 3$, via Newton method. With MAPLE 6, we can plot the discrete orbits $\{x[k]\} \subset R^3$, the discrete Poincaré projections

$$\left(\frac{x_i[k+1]+x_i[k]}{2}, \frac{x_i[k+1]-x_i[k]}{h}\right), \quad i = 1, 2, 3$$

and the graph $(k, \mathcal{H}[k])$ of the discrete Hamiltonian energy

$$\mathcal{H} = h^2\mathcal{H}_d(x[k-1], x[k]) = \frac{1}{2}\sum_{i=1}^{3}(x_i[k] - x_i[k-1])^2 - h^2 f\left(\frac{x[k]+x[k-1]}{2}\right).$$

Now let us accept that the discrete magnetic geometric dynamics is governed by the discrete Lagrangian

$$L_d(x[k-1], x[k]) = \frac{1}{2}\sum_{i=1}^{3}(x_i[k] - x_i[k-1])^2 + h^2 f\left(\frac{x[k]+x[k-1]}{2}\right).$$

Using the general form of the variational integrator [43], we write the discrete Euler-Lagrange equations as follows

$$x_i[k+1] - x_i[k] - \frac{h^2}{2}\frac{\partial f}{\partial x_i}\left(\frac{x[k+1]+x[k]}{2}\right) - A_i[k] = 0,$$

where the term $A_i[k]$ has the following expression

$$A_i[k] = x_i[k] - x_i[k-1] + \frac{h^2}{2}\frac{\partial f}{\partial x^i}\left(\frac{x[k]+x[k-1]}{2}\right).$$

Of course, if we denote

$$\varphi_i(u) = u_i - x_i[k] - \frac{h^2}{2}\frac{\partial f}{\partial x_i}\left(\frac{u+x[k]}{2}\right) - A_i[k],$$

the discrete solution is obtained by solving at each step k, the system of equations $\varphi_i(u) = 0$, $i = 1, 2, 3$, via Newton method. With MAPLE 6, we can plot the discrete orbits $\{x[k]\} \subset R^3$, the discrete Poincaré projections

$$\left(\frac{x_i[k+1]+x_i[k]}{2}, \frac{x_i[k+1]-x_i[k]}{h}\right), \quad i = 1, 2, 3$$

and the graph $(k, \mathcal{H}[k])$ of the discrete Hamiltonian energy

$$\mathcal{H} = h^2\mathcal{H}_d(x[k-1], x[k]) = \frac{1}{2}\sum_{i=1}^{3}(x_i[k] - x_i[k-1])^2 - h^2 f\left(\frac{x[k]+x[k-1]}{2}\right).$$

4 Simulation with MAPLE 6

The intention of this section is to illustrate the morphology of the magnetic field $\bar{H}_{Tr}$ respectively $\bar{H}_{Ga}$ which approximate the total magnetic field around the Ioffe-Ştefănescu configuration, using a specialized MAPLE 6 software realized in our Laboratory of Mathematical Visualization and Computer Graphics. All the simulation confirm and highlights the ideas of Ioffe-Ştefănescu, puting the reader at the forefront of current research in Magnetic Geometric Dynamics via computer experiments and computer graphics. They refer to phase portrait, level sets of density of magnetic energy trajectories in the magnetic geometric dynamics, Poincaré sections, and fields surfaces for $\bar{H}_{Tr}$ and $\bar{H}_{Ga}$ (the results contained in Figs.2-20 belong to this Section).

Acknowledgements. I want to thank Prof. Dr. Ion M. Popescu for the discussions we had on the magnetic traps, and to Prof. Dr. Mihai Postolache for his enthusiastic collaboration to the MAPLE simulations. The paper was supported by MEN Grant-21815/28.09.98, CNCSU-31.

References

[1] S. Bobbio: Struttura topologica dei campi magnetici nelle esperienze di fusione termonucleare controllata, *Notitiario della Unione Matematica Italiana*, Cagliari, 1-3 Gugne, 1987.

[2] C. Dumitrescu: Geometrical and topological structure of magnetic fields generated by rectilinear wires, PhD Thesis, University Politehnica of Bucharest, 1999.

[3] Yu.V.Gott, M.S.Ioffe, V.G.Tel'kovskii, Nucl.Fusion, 1962 Suppl., Part 3, p. 1045, 1962.

[4] N. A. Krall, A. W. Trivelpiece, Principles of Plasma Physics, McGraw-Hill Book Company, 1973.

[5] L. Milea: On the magnetic field lines of D. C. polygonal circuits, *Rev. Roum. Sc Tech. Electrotech., Energ.*, **31** (1986), 355-364.

[6] A. I. Morozov, L. S. Soloviev: The stucture of the magnetic fields, *Reviews of Plasma Physics*, Ed. M.A Leontovich, Vol. 2, Consultants Bureau, N.Y. (1966)

[7] S. Ştefănescu: Lignes du champ magnetique autour d'une ramification de courants, *Bull. Math. Phys. Pures et Appl.*, **1-9** (1925).

[8] S. Ştefănescu: Pour la prospection électrique du sous-sol. Noté présentée á l' Académie Roumanie (1927).

[9] S. Ştefănescu: Pour la prospection électrique du sous-sol; étude du champ S normal. Noté présentée á l'Académie Roumanie (1928).

[10] S. Ştefănescu: Lignes de champ magnétique d'un circuit filiforme, symetrique et plan, deux fois coudé, *Bull. Math. Pures et Aplliquées*, **1**, **2** (1935-1936), 19-20.

[11] S. Ştefănescu: Un nouveau cas d'application en électromagnétisme des fonctions cylindrique générales, *Bull. Math. Pures et Aplliquées*, 1, 2, 2: 22, 23, 24 (1936-1937).

[12] S. Ştefănescu: Un cas particullier des lignes H algébrique, *Bull. Math. Pures et Aplliquées*, 1, 2, 3: 25, 26, 27, 1-7 (1937-1938).

[13] S. Ştefănescu: Liniile de câmp magnetic ale unui curent electric filiform şi plan de două ori cotit, *Comunicările Academiei*, **1** No. 8 (1951), 769-774.

[14] S. Ştefănescu: Liniile de câmp magnetic ale poligoanelor regulate de curenţi rectilinii (I), *St. Cerc. Fiz.*, **5** No. 1-2 (1954), 63-70.

[15] S. Ştefănescu: Liniile de câmp magnetic ale poligoanelor regulate de curenţi rectilinii (II), *St. Cerc. Fiz.*, **6** No. 3 (1955), 459-471.

[16] S. Ştefănescu: Asupra unor linii de câmp magnetic definite prin transcendenţe elementare, *St. Cerc. Fiz.*, **7** No. 4 (1956), 519-530.

[17] S. Ştefănescu: Les lignes de champ magnétique d'un triangle de courants rectilignes, *Revue de Physique*, **1** (1956), 89-102.

[18] S. Ştefănescu: Open magnetic field lines, *St. Cerc. Fiz.*, **9** No. 1 (1958).

[19] S. Ştefănescu: Liniile de câmp magnetic ale unui curent directiliniu strâmb, *St. Cerc. Fiz.*, **10** (1959), 398-399.

[20] S. Ştefănescu, M. Nabighian: Magnetic field lines of two equal rectilinear currents, *St. Cerc. Fiz.*, **3** (1960), 563-583; *Rev. Roum. Géol. Géophys. et Géogr-Géophys*, **31** (1987), 95-112.

[21] S. Ştefănescu, M. Nabighian: Asupra liniilor de câmp magnetic ale emiţătorului AB, *Probleme de Geofizică*, **1** (1961), 181-186.

[22] S. Ştefănescu: Liniile de câmp magnetic împrejurul unei prize de pământ într-un teren cu stratificaţie paralelă, *Probleme de Geofizică*, **2** (1963), 135-145.

[23] S. Ştefănescu: Liniile de câmp ale unui dreptunghi centrat de curenţi rectilinii egali, *St. Cerc. Fiz.*, **21** No. 1 (1969), 21-32.

[24] S. Ştefănescu: Nouveaux exemples de lignes de champ magnétique ouvertes, *Rev. Roum. Phys.*, **15** No. 1 (1970), 11-25.

[25] S. Ştefănescu: Lignes de champ magnétiques d'un parallélogramme centré de courant rectilignes égaux (I), *Rev. Roum. Phys.*, **17** No. 9 (1972), 1041-1052.

[26] S. Ştefănescu: Lignes de champ magnétiques d'un parallélogramme centré de courant rectilignes égaux (II), *Rev. Roum. Phys.*, **18** No. 1 (1973), 35-48.

[27] S. Ştefănescu: Sur les lignes du champ magnétique d'un circuit électrique en forme de losange aplati, *Rev. Roum. Phys.*, **21** No. 4 (1976), 421-430.

[28] S. Ştefănescu: Sur les lignes du champ magnétique d'un ligne électrique bifilaire,plane symétriquement coudée, *Rev. Roum. Phys.*, **22** 9 (1977), 911-921.

[29] S. Ştefănescu: Open magnetic field lines (II), *Rev. Roum. Phys.*, **31** 7 (1986), 701-721.

[30] S. Ştefănescu: Addenda1987- Open magnetic field lines (III), *Rev. Roum. Géol., Géophys., Géogr.-Géophysique*, **31** (1987), 113-119.

[31] S. Ştefănescu: Une hobby mathématique, *Rev. Roum. Phys.*, **31** (1987), 89-93.

[32] S. Ştefănescu: Lignes H, circuits rectiligne coudés, *Manuscript Notices*, 1944-1992 unpublished.

[33] S. Ştefănescu and C. Udrişte: Magnetic field lines around filiform electrical circuits of right angle type, *Sci. Bull. P.U.B. Series A: Appl. Math. Phys.*, **55** (1993), 3-18.

[34] A. Udrişte: Geometric properties of magnetic field lines around two filiform electric circuits of right angle type, *Poster at The First European Congres of Math.*, Paris, July 6-10 (1992).

[35] A. Udrişte and C. Udrişte: Dynamics induced by a magnetic field, in Ed. J. Szenthe, "New Developments in Differential Geometry", Budapest 1996, pp. 429-442, Kluwer Academic Publishers, 1999.

[36] C. Udrişte: Linii de câmp, *E. T. Bucureşti*, 1988.

[37] C. Udrişte: Asupra conjecturii Acad. S. Ştefănescu, Probleme actuale ale geometriei, Romanian Academy (1989).

[38] C. Udrişte: *Geometric Dynamics*, Southeast Asian Bulletin of Mathematics, Springer-Verlag 24 (2000), 313-322; Kluwer Academic Publishers, Dordrecht/Boston/London, Mathematics and Its Applications, 513, 2000.

[39] C. Udrişte: Discrete geometric dynamics, in Proc. First French-Romanian Coll. of Num. Physics, October 30-31, 2000, Univ. Politehnica of Bucharest, Geometry Balkan Press, Romania.

[40] C. Udrişte and M. Postolache (Eds.); Magnetic fields generated by filiform electric circuits, *Geometry Balkan Press*, Bucharest, 1999.

[41] C. Udrişte and M. Postolache: Least squares problem and geometric dynamics, *Ital. J. Pure Appl. Math.*, **15** (2000) (in printing).

[42] C. Udrişte and M. Postolache: Least squares problem and magnetic dynamics, in *Global Analysis, Differential Geometry and Lie Algebras* (Gr. Tsagas (Ed.)); Workshop on Global Analysis, Differential Geometry and Lie Algebras, Thessaloniki, June 24-28 (2000); pp. 169-238, 2000.

[43] C. Udrişte and M. Postolache: Atlas of Magnetic Geometric Dynamics, *Geometry Balkan Press*, Bucharest, 2001.

[44] C. Udrişte, M. Postolache and A. Soeanu: Computer simulation of magnetic phase portraits around piecewise rectilinear circuits; in *Global Anal., Diff. Geom. and Lie Algebras*, (Edited de Gr. Tsagas), Geometry Balkan Press, 1999, pp. 130-140.

[45] C. Udrişte, M. Postolache and A. Udrişte: Acad. Sabba Ştefănescu conjecture; lines of magnetic field generated by filiform electrical circuits; *Rev. Roum. Geoph.*, **36** (1992), 17-25.

[46] C. Udrişte, M. Postolache and I. Ţevy: Integrator for Lagrangian dynamics, *Balkan J. Geom. Appl.*, **6** No. 2(2001), 109-115.

[47] C. Udrişte, M. Postolache and A. Udrişte: Energy of magnetic field generated by currents through filiform electrical circuits of right angle type; *Tensor, N.S.*, **54** (1993), 185-196.

[48] C. Udrişte, M. Postolache and A. Udrişte: Numerical simulation of dynamic magnetical system; *U.P.B. Sci. Bull. Series A: Appl. Math. Phys.*, **55** No. 1-2 (1993), 51-64.

[49] C. Udrişte, M. Postolache, T. Mazilu and A. Udrişte; Equilibrium sets of magnetic fields around electric circuits; in *Global Anal., Diff. Geom. and Lie Algebras*, (Edited by Gr. Tsagas), Geometry Balkan Press, 1998, pp. 125-136.

[50] C. Udrişte, A. Udrişte, V. Balan and M. Postolache: Magnetic field generated by two coplanar electrical circũits of fixed angle type and its field lines; in *Proc.* 24^{th} *Conf. Geom. Topol.*, Timişoara, 1994, pp. 285-301.

[51] C. Udrişte, A. Udrişte, V. Balan and M. Postolache: Magnetic dynamical systems; *An. Şt. "Al. I. Cuza" Univ.*, Iaşi, Tom 4, Informatică, 1995, pp. 105-126.

[52] C. Udrişte, A. Udrişte, V. Balan and M. Postolache: Equilibrium points of magnetic fields generated around filiform electrical circuits, *Tensor, N.S.*, **57** (1996), 119-134.

[53] C. Udrişte, A. Udrişte, V. Balan and M. Postolache: Phase portraits and critical elements of magnetic fields generated by piecewise rectilinear electrical circuits, *Fundam. Theor. Phys.*, **76** (1996), 177-186, Kluwer, (Lagrange and Finsler Geometry (P.L. Antonelli and R. Miron (Eds)).

Author's address:

C. Udrişte *Politehnica University of Bucharest, Department of Mathematics I Splaiul Independenţei 313, 77206 Bucharest, Romania E-mail: udriste@mathem.pub.ro*

FIG.1. IOFFE-STEFANESCU CONFIGURATION

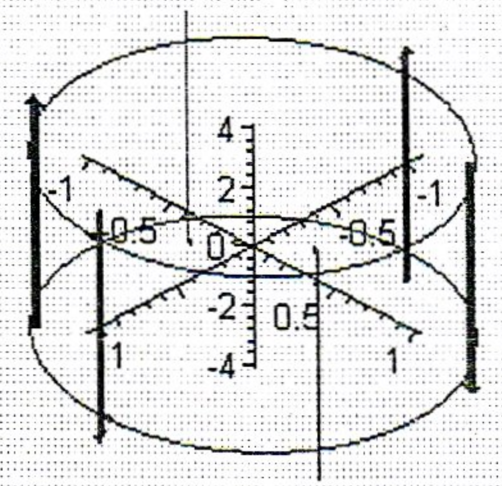

Schematic of a current distribution that produces a magnetic field having the property of increasing in all directions outward from the center. Multipole windings are called Ioffe-Stefanescu bars, after Ioffe, who first used them in experiments that suppressed the hydromagnetic instabilities in a magnetically confined plasma, and after Stefanescu, who first claimed that a suitable magnetic field can be obtained using an appropriate geometry for the electric configuration.

FIG.2. IOFFE-STEFANESCU MAGNETIC PHASE PORTRAIT
(TRAPEZOIDAL APPROXIMATION)

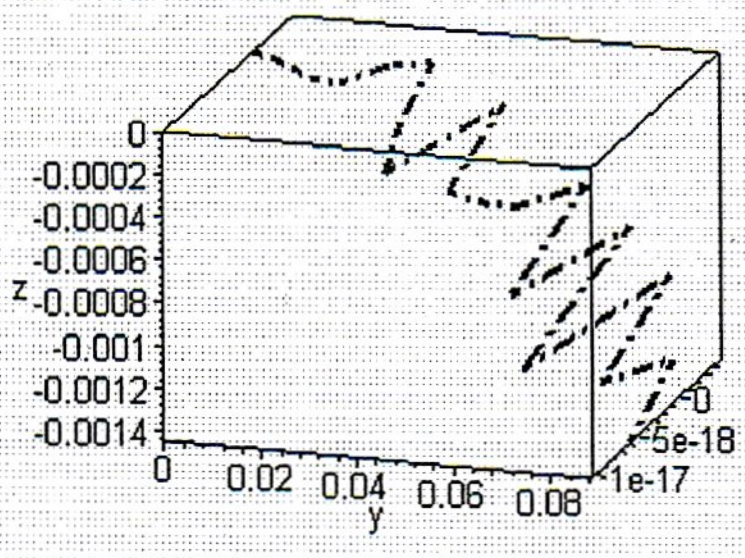

([x(0)=0,y(0)=0,z(0)=0],stepsize=.1,linestyle=4,method=rkf45,linecolor=t,maxfun=30000)

FIG.3. IOFFE-STEFANESCU MAGNETIC PHASE PORTRAIT
(THREE POINTS GAUSS APPROXIMATION)

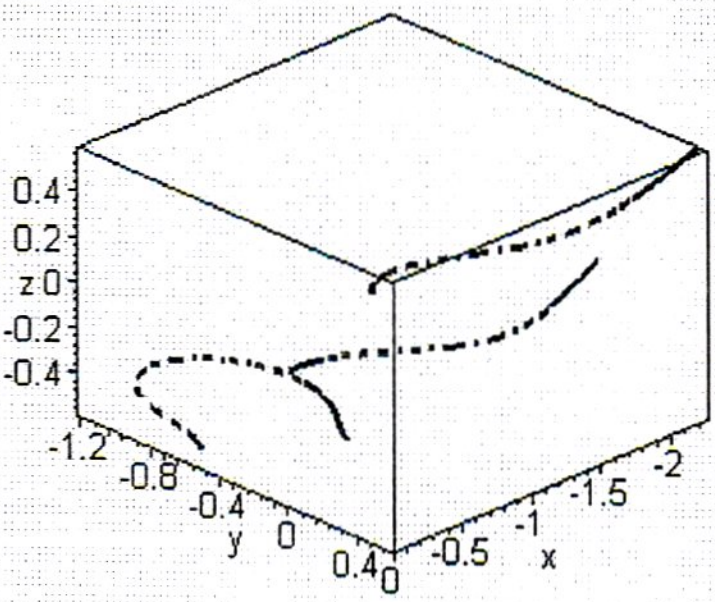

([x(0)=0,y(0)=0,z(0)=0],[x(0)=0,y(0)=0.5,z(0)=0.5],[x(0)=0,y(0)=-0.5,z(0)=-0.5],
stepsize=.1,linestyle=4, method=rkf45,linecolor=t,maxfun=30000)

FIG.4. LEVEL=.01 SET OF IOFFE-STEFANESCU ENERGY
DENSITY (TRAPEZOIDAL APPROXIMATION)

implicitplot3d(f=.01, x=-0.5..0.5, y=-0.5..0.5, z=-0.5..0.5, grid=[25,25,25])

FIG.5. LEVEL=1 SET OF IOFFE-STEFANESCU ENERGY DENSITY (TRAPEZOIDAL APPROXIMATION)

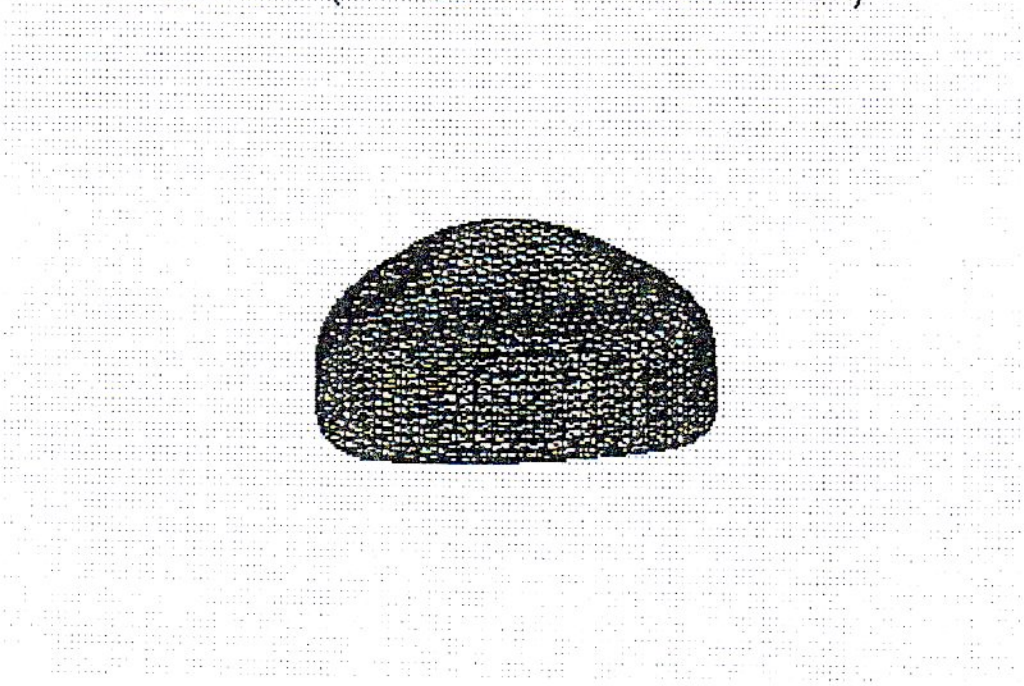

implicitplot3d(f=1, x=-0.5..0.5, y=-0.7..0.7, z=-3.5..3.5, grid=[25,25,25])

FIG.6.LEVEL=1 SET OF IOFFE-STEFANESCU ENERGY DENSITY (THREE POINTS GAUSS APPROXIMATION)

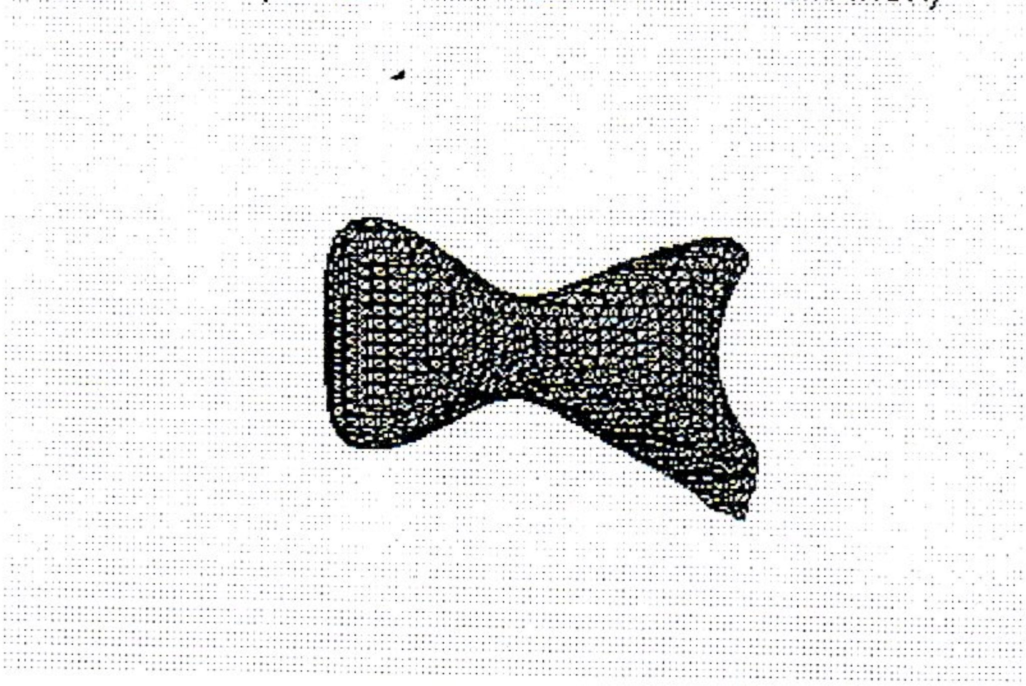

implicitplot3d(f=1, x=-0.7..0.7, y=-0.7..0.7, z=-2.5..2.5, grid=[25,25,25])

FIG.7. LEVEL=0.05 SET OF IOFFE-STEFANESCU ENERGY DENSITY (THREE POINTS GAUSS APPROXIMATION)

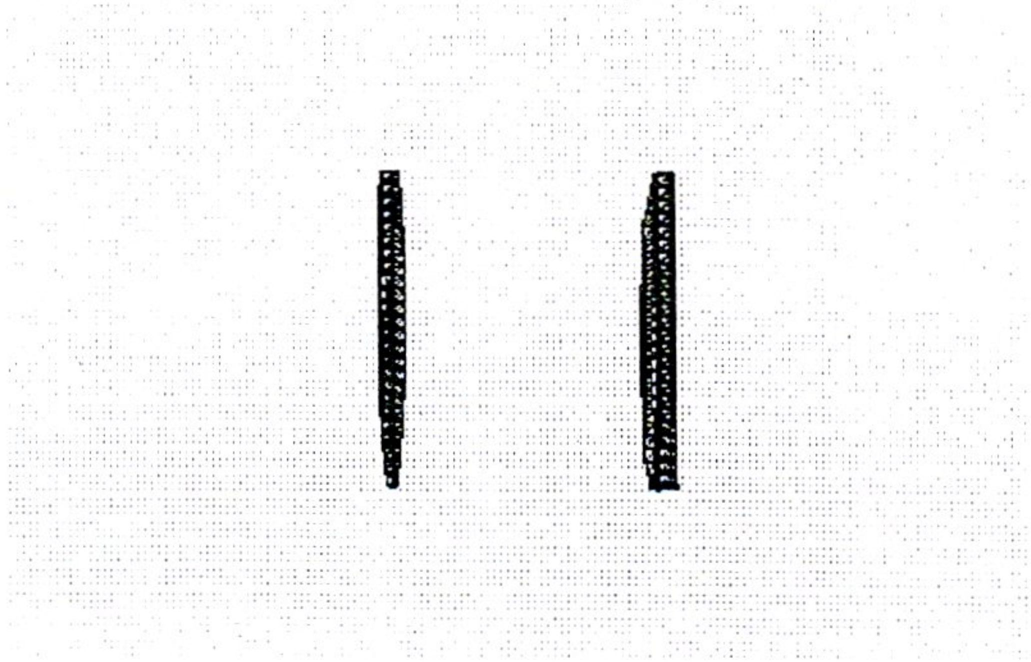

implicitplot3d(f=.05, x=-0.7..0.7, y=-0.7..0.7, z=-0.5..0.5, grid=[25,25,25])

FIG.8. GRAPH OF f(x,0,0)

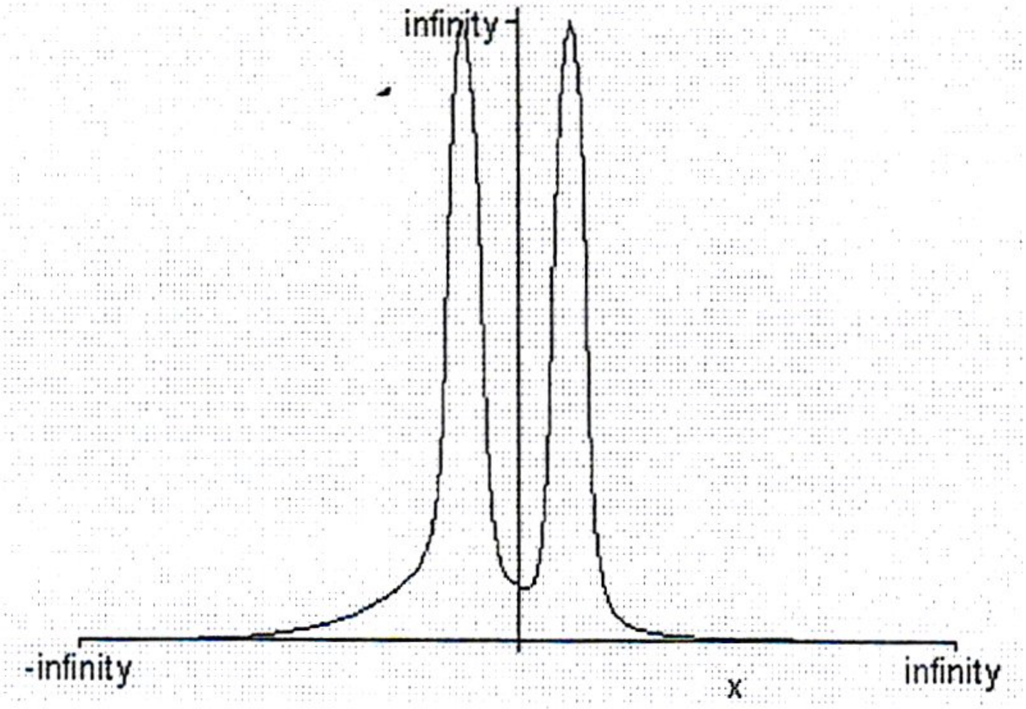

FIG.9. GRAPH OF f(0,y,0)

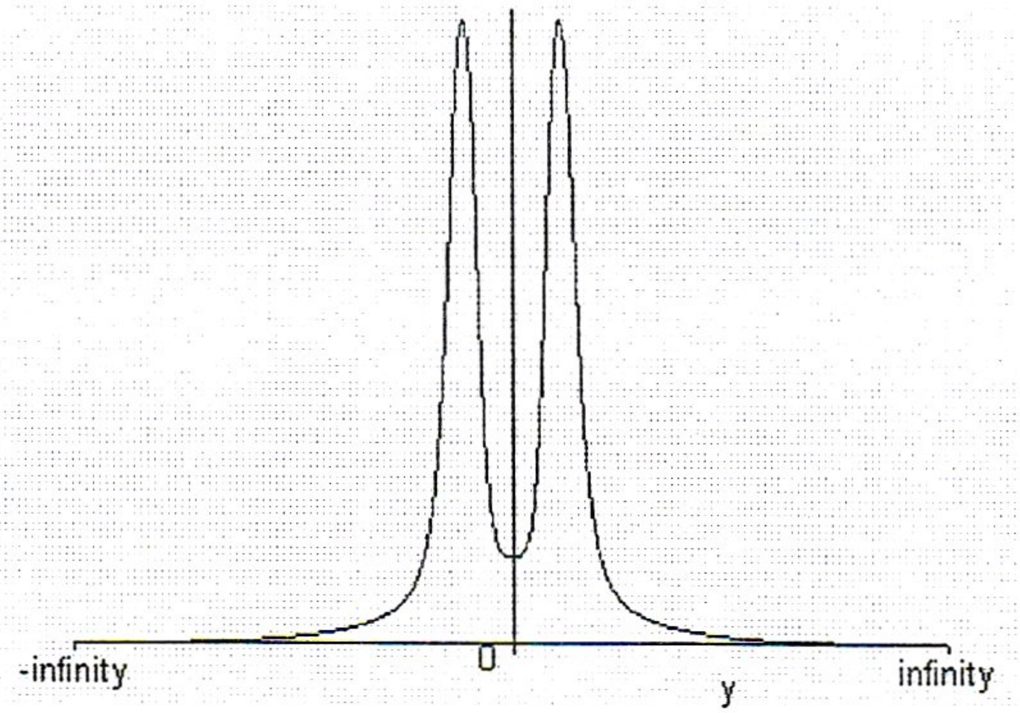

FIG.10. GRAPH OF f(0,0,z)

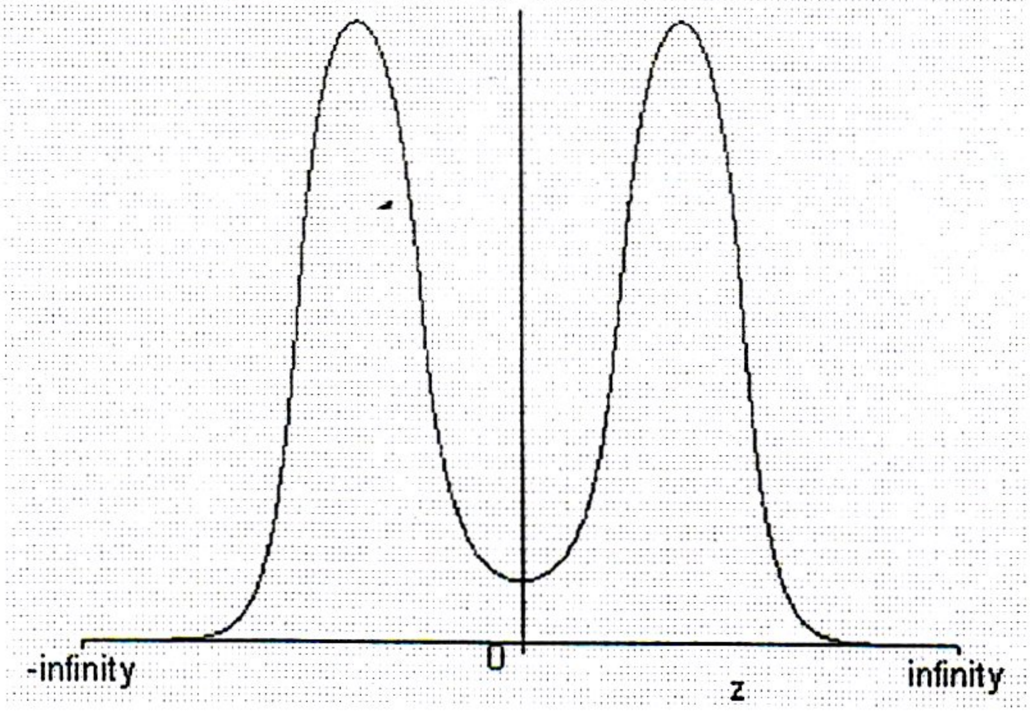

FIG.11. GRAPH OF f(x,y,0)

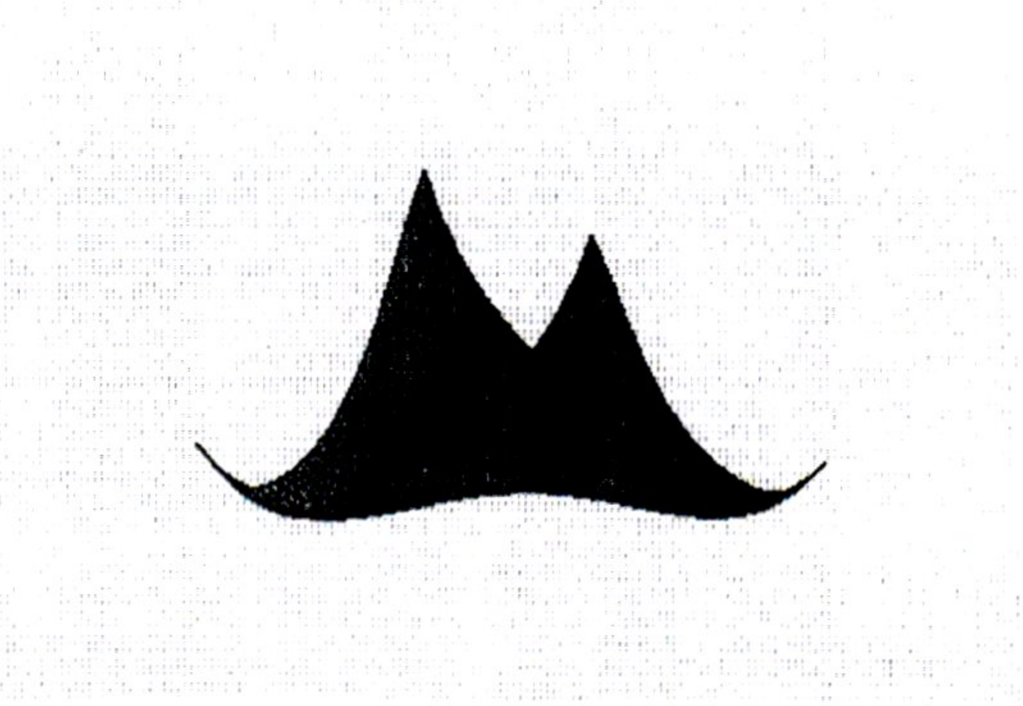

plot3d(f(x,y,0), x=-0.5..0.5, y=-0.5..0.5)

FIG.12. LEVEL CURVES OF f(x,y,0)

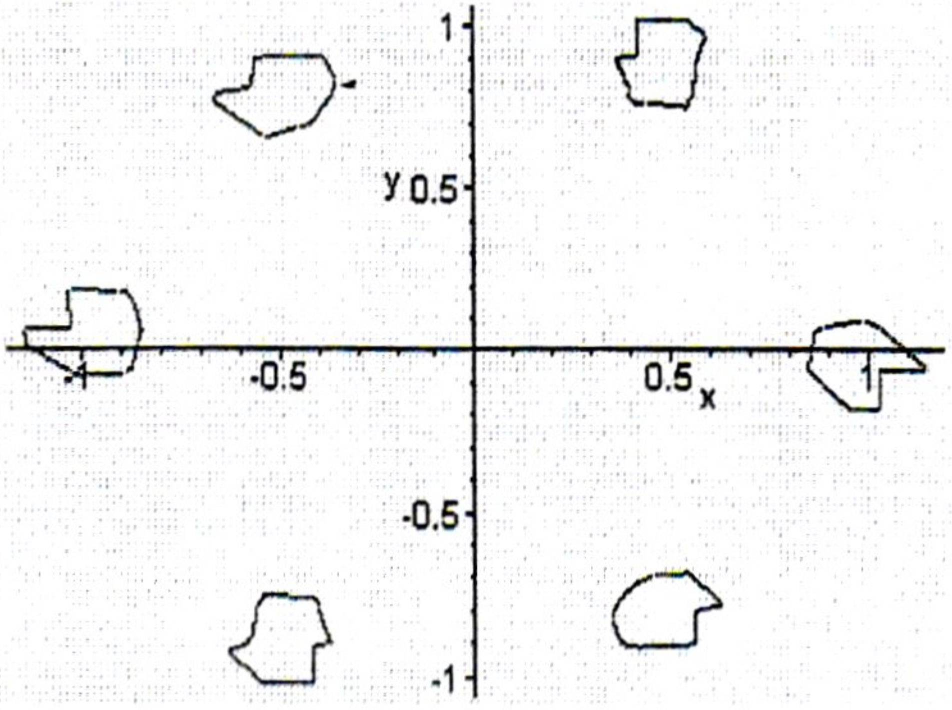

implicitplot(f(x,y,0)=20, x=-1.5..1.5, y=-1.5..1.5)

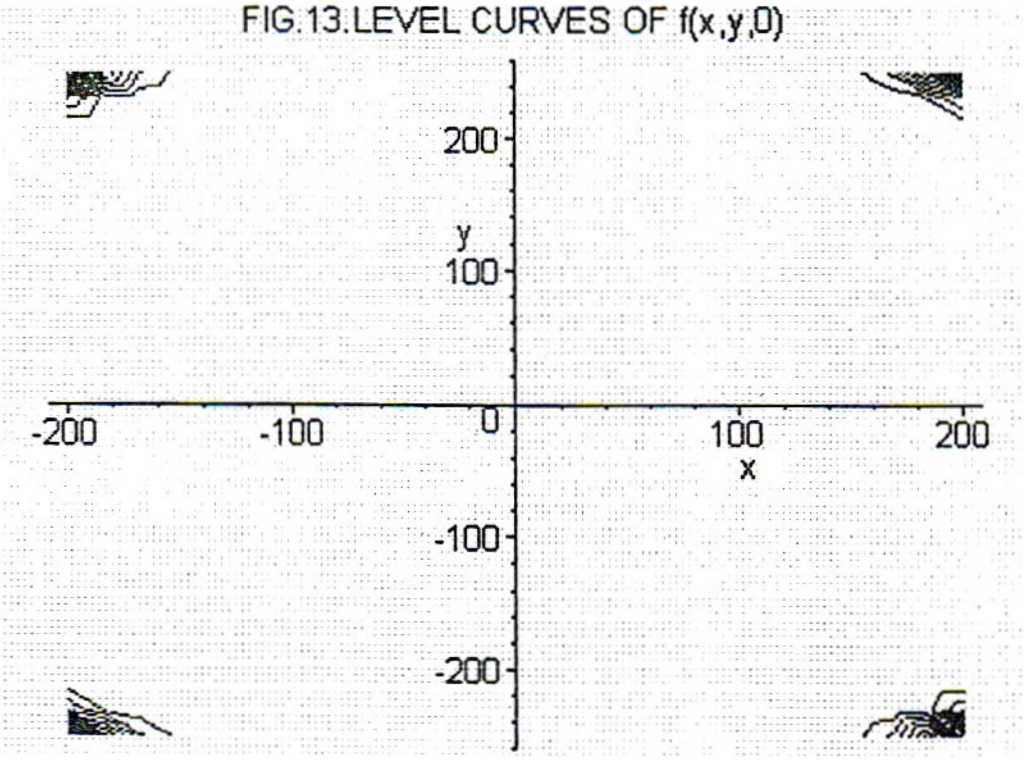

contourplot(f(x,y,0), x=-200..200, y=-250..250, contours=20)

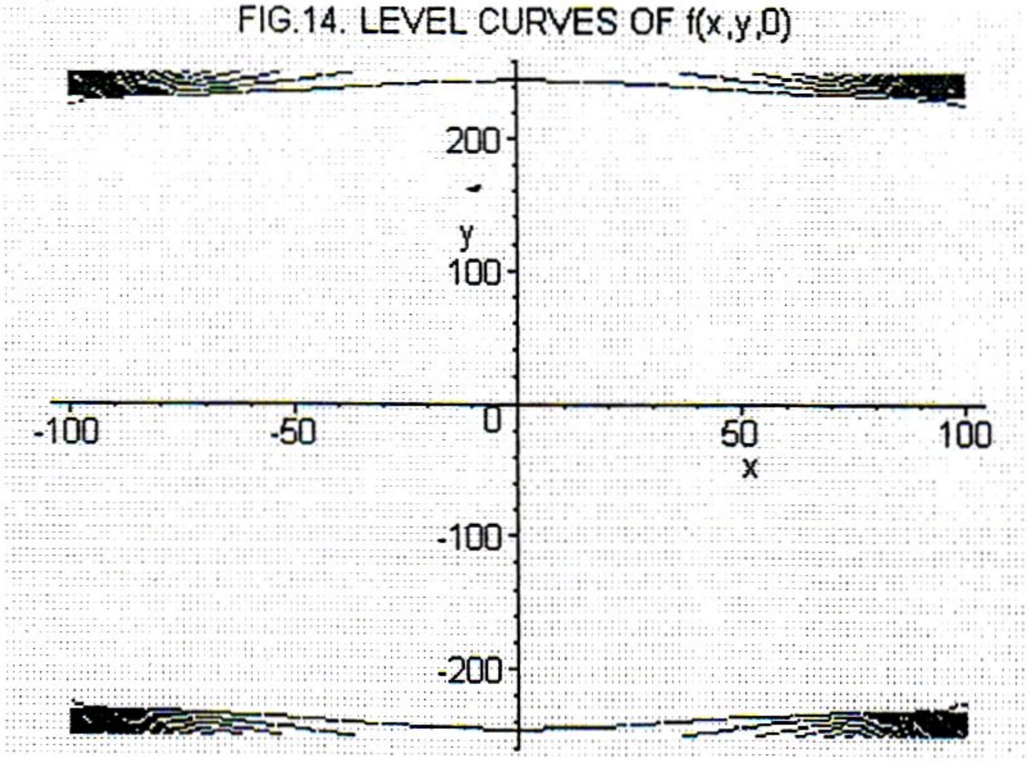

contourplot(f(x,y,0), x=-100..100, y=-250..250, contours=20)

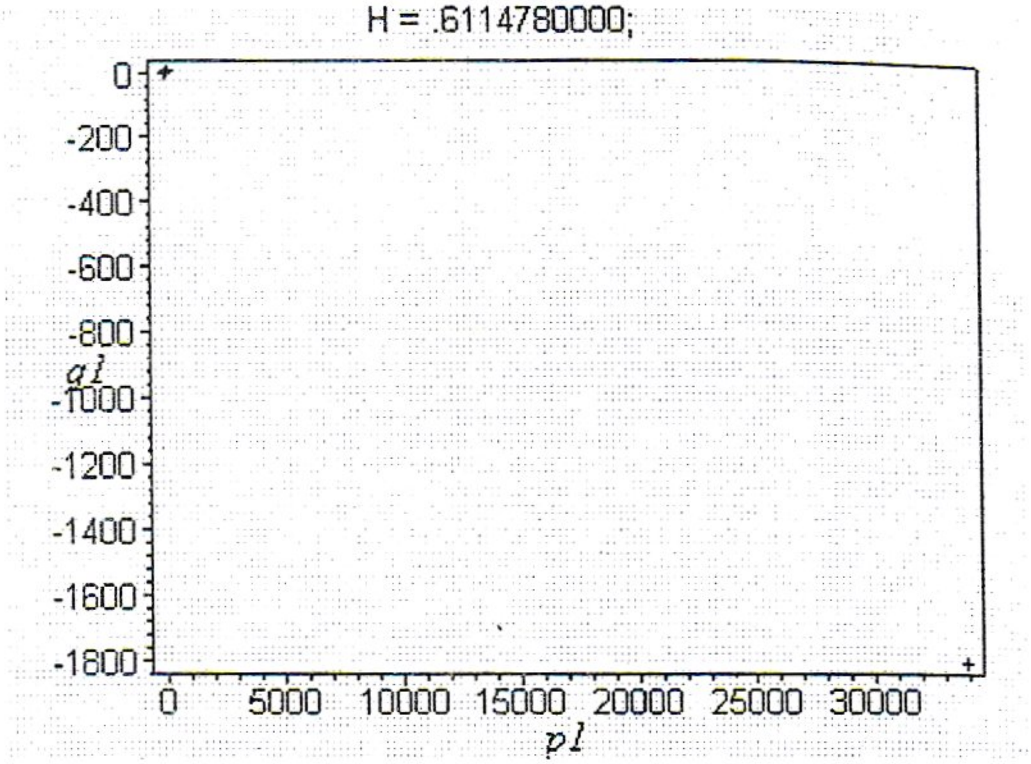

Fig.15. Trapezoidal approximation; poincare(H,t=-10..10, {[0,1,-1,0,0,0,1.5]}, stepsize=0.1, iterations=30)

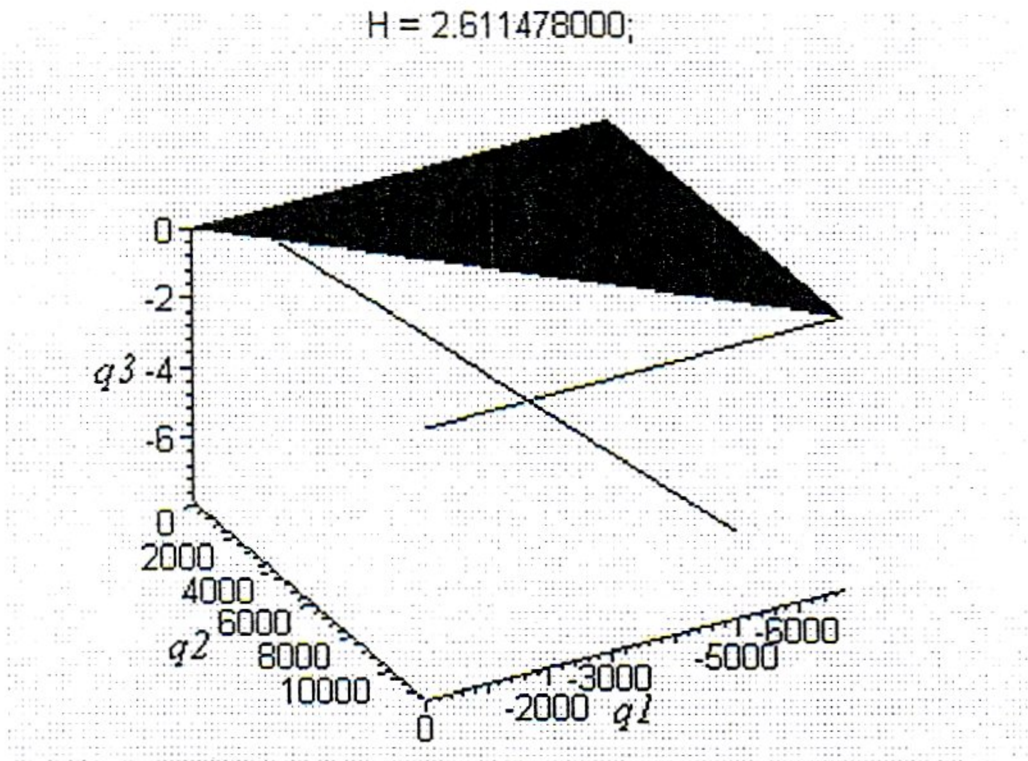

Fig.16. Trapezoidal approximation; poincare(H,t=-10..10, {[0,1,2,1,0,0,1.5]}, stepsize=0.1, iterations=30,3)

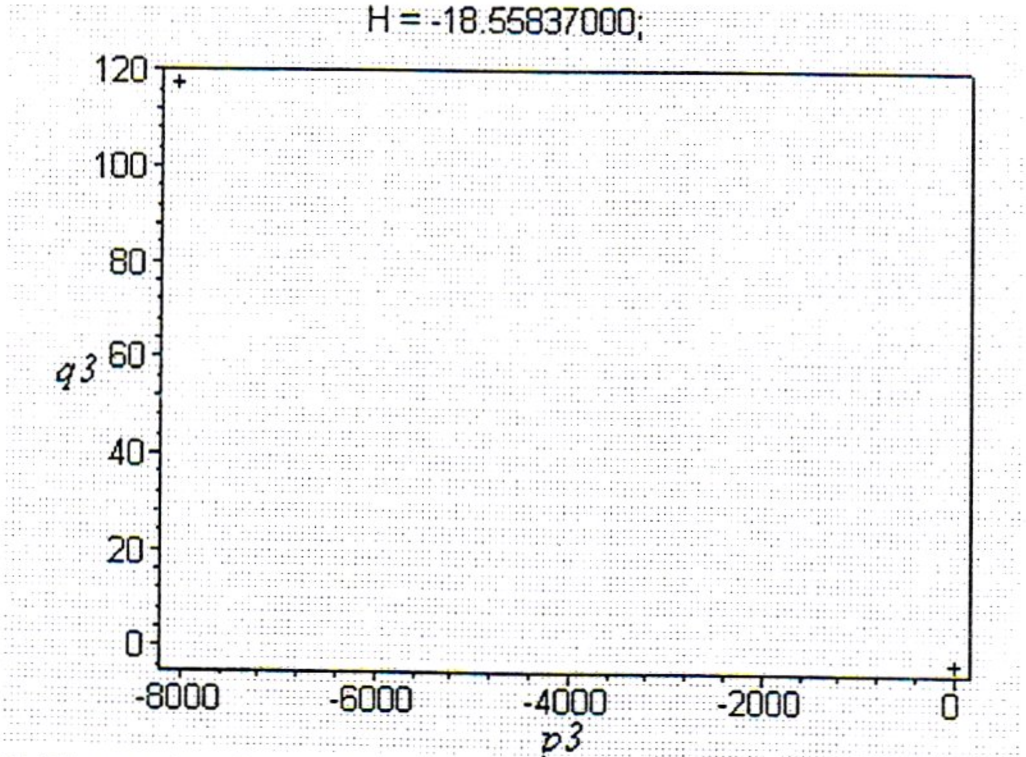

Fig.17. Three points Gauss approximation; poincare (H,t=-1..1, {[0,1,1,0,0,0,-3]}, stepsize=0.05, iterations=30)

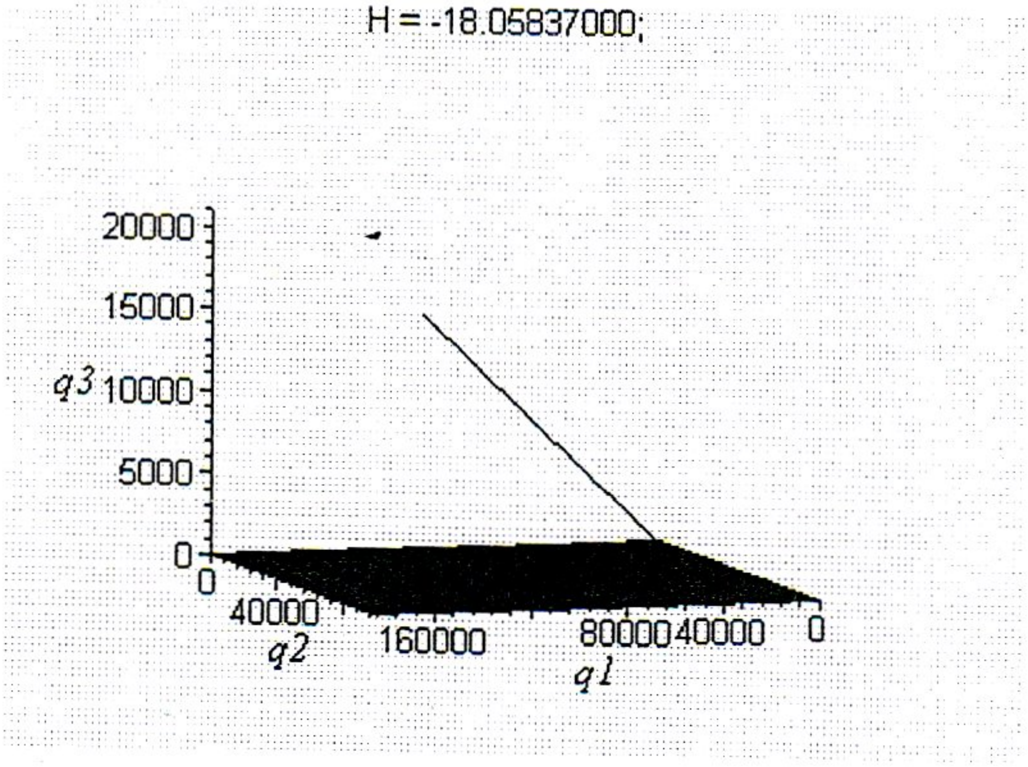

Fig.18. Three points Gauss approximation; poincare (H,t=-1.5..1.5, {[0,1,1,1,0,0 3]}, stepsize=0.05, iterations=30,3)

FIG.19. IOFFE-STEFANESCU MAGNETIC SURFACE: u(x,y,z)=0
(TRAPEZOIDAL APPROXIMATION)

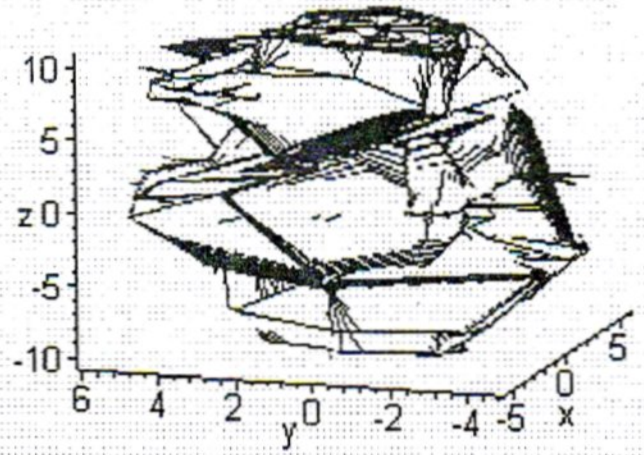

ics:=[0.5*cos(t),0.5*sin(t),s,t], t=-Pi..Pi, s=-10..10, numchar=[10,10], iterations=25, numsteps=[20,20], stepsize=.15, initcolor=t

FIG.20. IOFFE-STEFANESCU MAGNETIC SURFACE: u(x,y,z)=0
(THREE POINTS GAUSS APPROXIMATION)

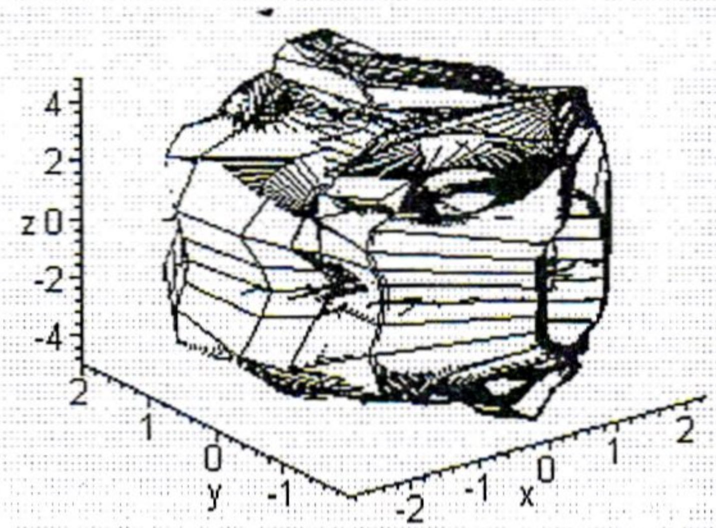

ics:=[1.5*cos(t),1.5*sin(t),s,t], t=-Pi..Pi, s=-4..4, numchar=[15,15], iterations=50, numsteps=[20,20], stepsize=.001, initcolor=t